HOKKAIDO UNIVERSITY

Title	Coexistence of High Electron Conduction and Low Heat Conduction in Tungsten Oxide Epitaxial Films with 1D Atomic Defect Tunnels
Author(s)	Kim, Gowoon; Feng, Bin; Sheu, Yu-Miin et al.
Citation	ACS Applied Electronic Materials, 2(8), 2507-2513 https://doi.org/10.1021/acsaelm.0c00428
Issue Date	2020-08-25
Doc URL	https://hdl.handle.net/2115/82516
Rights	This document is the Accepted Manuscript version of a Published Work that appeared in final form in ACS Applied Electronic Materials, copyright © American Chemical Society after peer review and technical editing by the publisher. To access the final edited and published work see https://pubs.acs.org/doi/10.1021/acsaelm.0c00428 .
Type	journal article
File Information	Supplymentary_ACS Appl. Electron. Mater._ver1_HOrev.pdf, Supporting Information

Hokkaido University Collection of Scholarly and Academic Papers : HUSCAP

Supporting Information

Coexistence of High Electron Conduction and Low Heat Conduction in Tungsten Oxide Epitaxial Films with 1D Atomic Defect Tunnels

Gowoon Kim*[,1], Bin Feng[2], Yu-Miin Sheu[3], Hai Jun Cho[1,4], Yuichi Ikuhara[2], and Hiromichi Ohta*[,1,4]

[1]Graduate School of Information Science and Technology, Hokkaido University, N14W9, Kita, Sapporo 060−0814, Japan

[2]Institute of Engineering Innovation, The University of Tokyo, 2−11−16 Yayoi, Bunkyo, Tokyo 113−8656, Japan

[3]Center for Emergent Functional Matter Science, National Chiao Tung University, Hsinchu, 30010, Taiwan

[4]Research Institute for Electronic Science, Hokkaido University, N20W10, Kita, Sapporo 001−0020, Japan

***Corresponding Authors**

Gowoon Kim email: rlarhdns32@eis.hokudai.ac.jp

Hiromichi Ohta email: hiromichi.ohta@es.hokudai.ac.jp

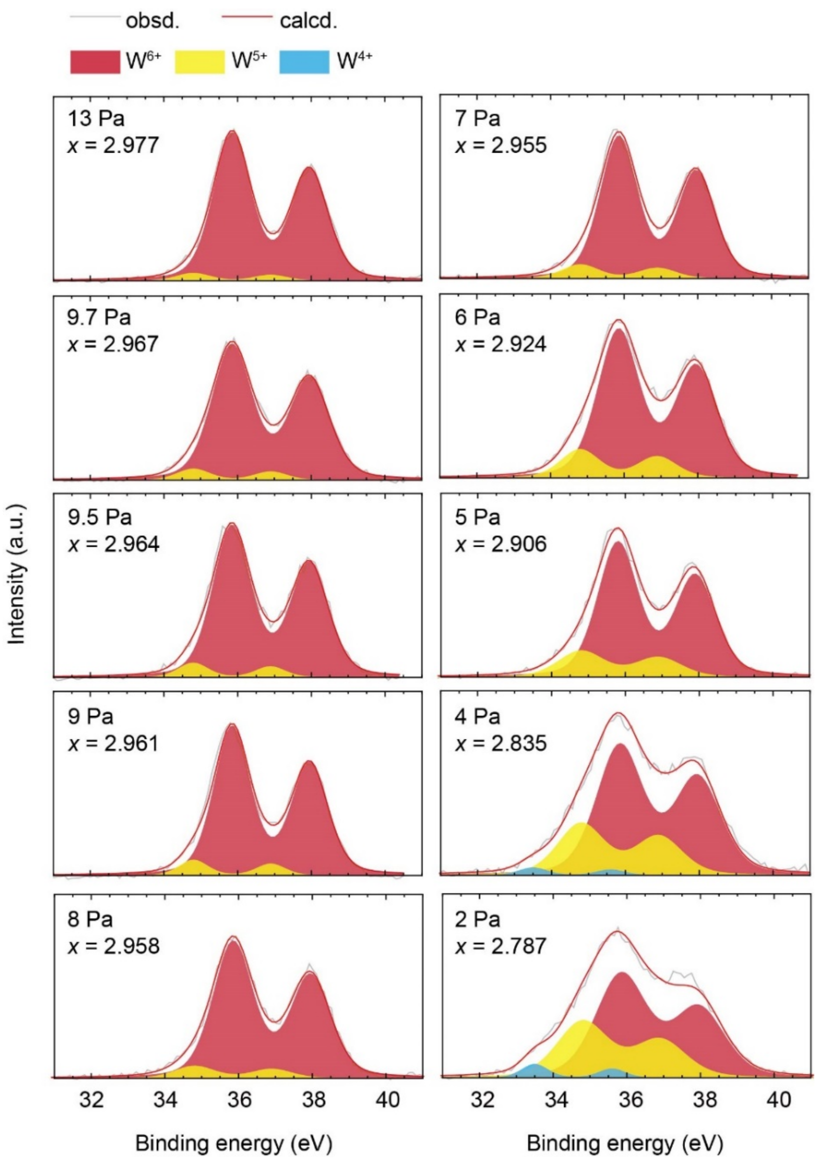

Figure S1. XPS spectra around the W 4f peaks of the WO_x thin films. Both W $4f_{7/2}$ (~36 eV) and W $4f_{5/2}$ (~38 eV) peak width becomes broader with decreasing the oxygen pressure (P_{O2}) during the film growth. The observed spectra are de-convoluted by W^{6+}, W^{5+}, and W^{4+} valence states. The calculated spectra are matched well with the observed spectra in all cases.

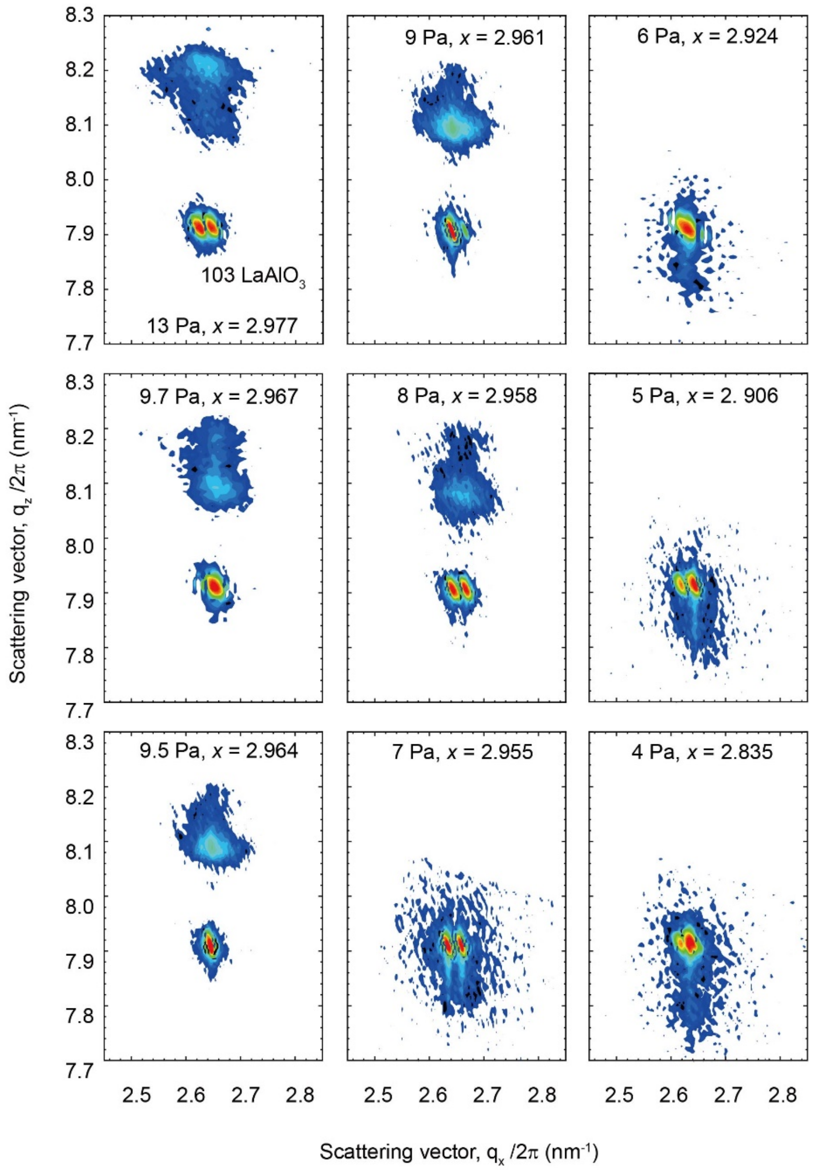

Figure S2. X-ray reciprocal space mappings (RSMs) of the WO_x films. The diffraction spots of WO_x locate at the same $q_x/2\pi$ position with that of 103 $LaAlO_3$ substrates, indicating coherent epitaxial growth occurred in all cases.

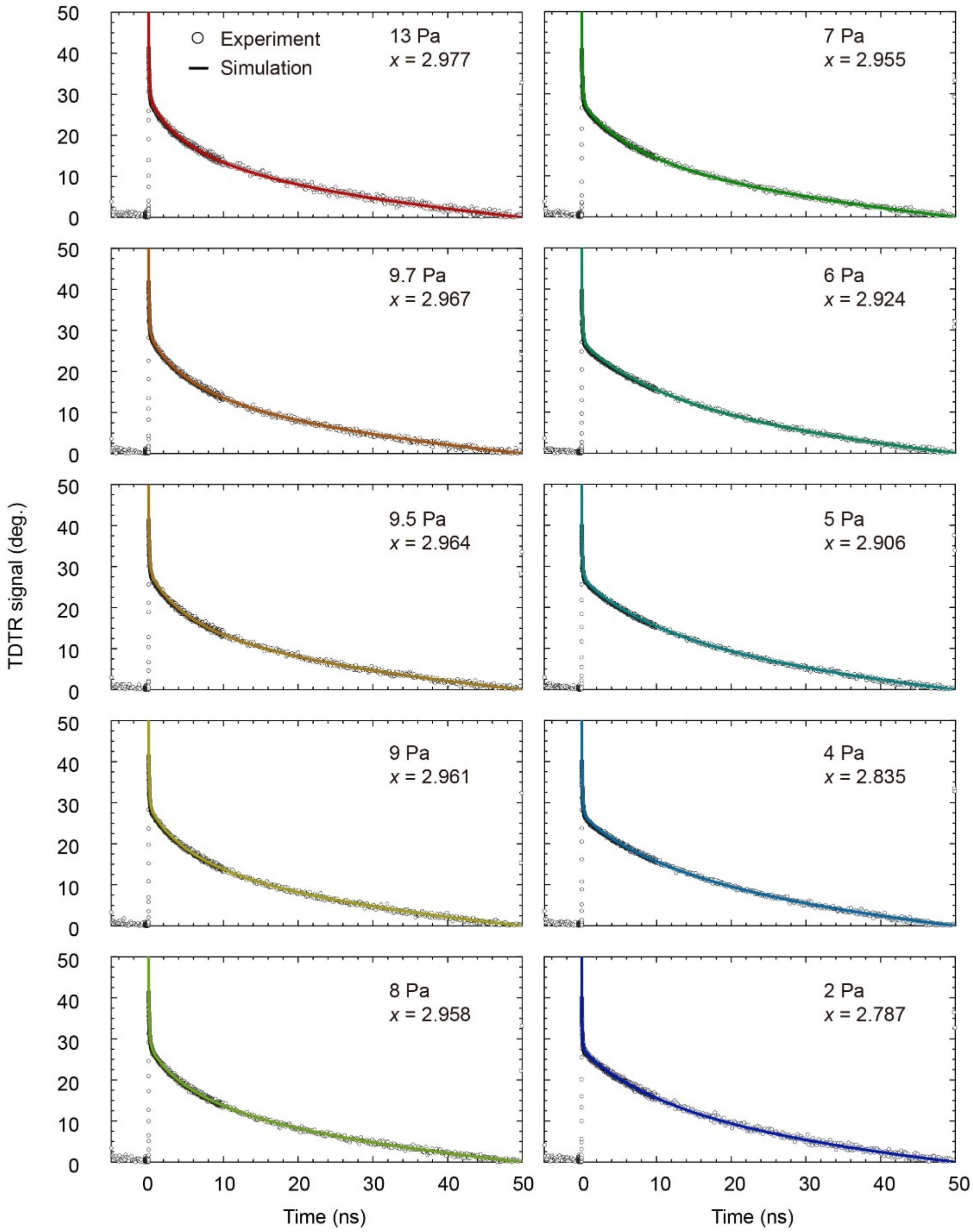

Figure S3. The time-dependent decay curves of the TDTR phase signal and fitted curve for WO_x epitaxial films. Simulation layers are composed of 116 nm-thick Mo/ 40-nm-thick WO_x / $LaAlO_3$ substrate three-layers. The sharp increase of signal from 0 ns to 1 ns comes from Mo transducer. Experimentally obtained decay curve (circle) are simulated with varying thermal conductivity of WO_x films.

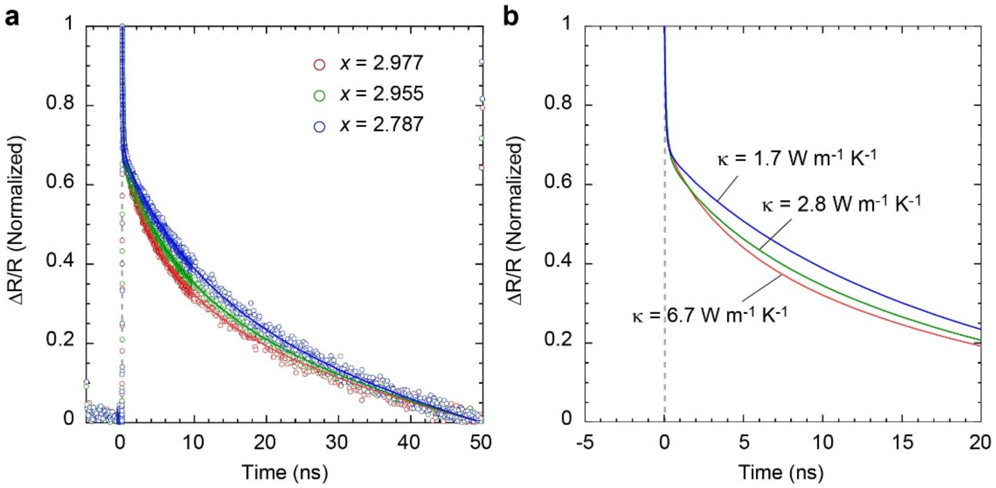

Figure S4. Normalized decay curve of the TDTR phase signal. (a) The thermal decay curves of $WO_{2.977}$, $WO_{2.955}$ and $WO_{2.787}$ display clear differences in thermal conductivity (κ) for various WO_x films. (b) The simulated κ are 6.7 W m^{-1} K^{-1} ($WO_{2.977}$), 2.8 W m^{-1} K^{-1} ($WO_{2.955}$) and 1.7 W m^{-1} K^{-1} ($WO_{2.787}$), respectively.

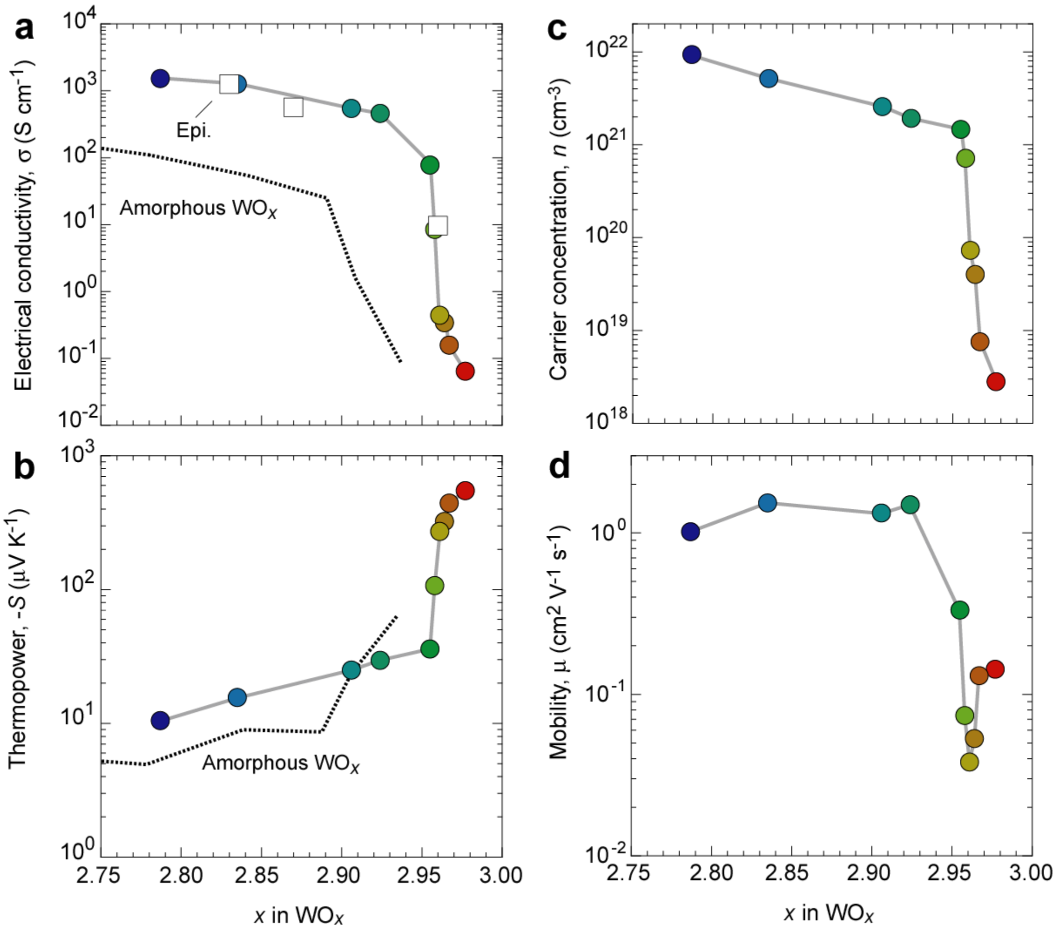

Figure S5. In-plane electron transport properties of the WO_x films. (a) Electrical conductivity (σ). Reported σ values of epitaxial WO_x film (white square)[1] and amorphous WO_x film (dotted line)[2] are also plotted. (b) The absolute values of the thermopower (S). (c) The carrier electron concentration (n). (d) The carrier mobility (μ). The carrier concentration values were extracted from the thermopower data (Fig. S6). All transport properties show drastic change with x ranging from 2.98 to 2.92. Note both carrier electron concentration and mobility increase with increasing 1D atomic defect tunnel.

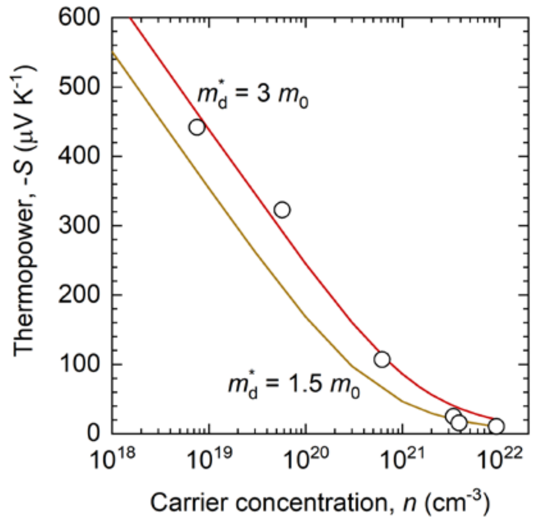

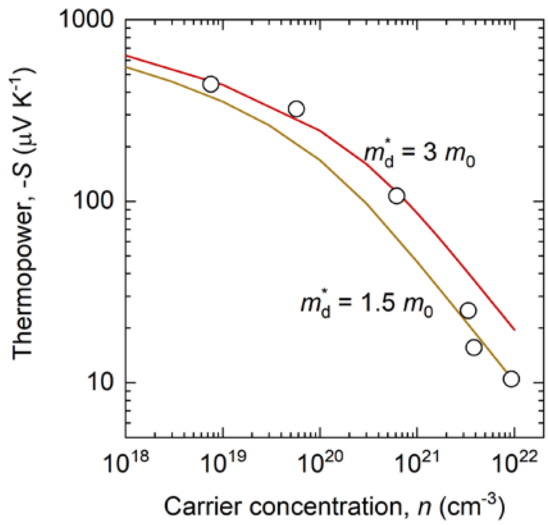

Figure S6. Calculated thermopower of WO_x epitaxial films as a function of the carrier concentration. Experimentally observed thermopower gives two different density of states effective masses (upper: The *y*-axis is linearly scaled. Lower: The *y*-axis is logarithmically scaled.). $n < 10^{21}$ cm^{-3}: $m_d^* = 3\ m_0$, $n > 10^{21}$ cm^{-3}: $m_d^* = 1.5\ m_0$. Details of the thermopower estimation have been described elsewhere.

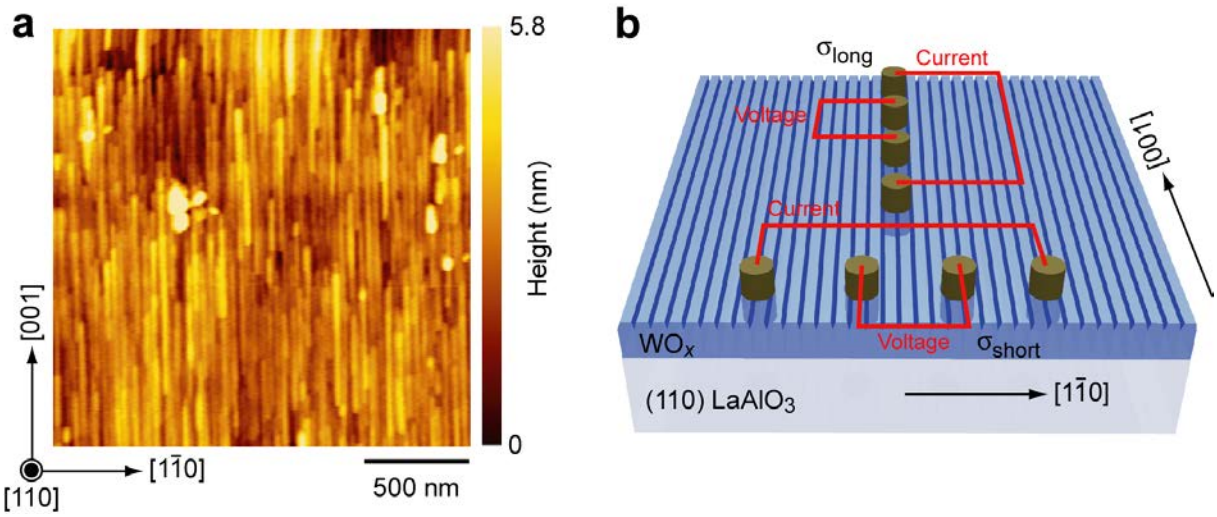

Figure S7. 1D electrical conductivity measurement of WO_x films with uniaxially oriented rectangular grains on (110) $LaAlO_3$ substrates. (a) Topographic AFM image (2 μm × 2 μm) of the $WO_{2.83}$ film grown on (110) $LaAlO_3$ substrate. Many rectangular-shaped grains (*L* ~600 nm, *W* ~20 nm) aligned in [001] direction are seen. (b) Schematic measurement direction of the electrical conductivity. 1D electrical conductivity was measured along [001] (σ_{long}) and [1-10] (σ_{short}) by d.c. four probe method.

REFERENCES

(1) Ning, S.; Huberman, S. C.; Ding, Z. W.; Nahm, H. H.; Kim, Y. H.; Kim, H. S.; Chen, G.; Ross, C. A., Anomalous defect dependence of thermal conductivity in epitaxial WO_3 thin films. *Adv. Mater.* **2019,** *31* (43), 1903738.

(2) Kim, G.; Cho, H. J.; Sheu, Y. M.; Ohta, H., Electrical, Optical, and Thermal Transport Properties of Oxygen-Deficient Amorphous WO_x ($2.5 < x < 3$) Films. *J. Phys. Chem. C* **2019,** *123* (25), 15419-15424.